

ON THE DETERMINATION OF THE MODULUS OF ELASTICITY OF WOOD BY COMPRESSION TESTS PARALLEL TO THE GRAIN

Xavier J.; Jesus, A.; Morais, J.; Pinto, J.
CITAB/UTAD, Vila Real, Portugal

ABSTRACT

*In this work, the determination of the longitudinal modulus of elasticity (E_L) of maritime pine (*Pinus Pinaster* Ait.) wood was investigated by means of compression test parallel to the grain. The effect of parasitic end-effects (i.e., friction and damage) on the correct evaluation of the E_L modulus was studied using parallelepiped wood specimens with different cross-section areas and lengths. The results from the data reduction conventionally applied to this test method were compared to values obtained from strain measurement provided by a full-field optical method (stereovision technique). The influence of the geometry of the specimen on the correct evaluation of the E_L was assessed and discussed.*

1- INTRODUCTION

At the macroscopic scale (10-200 mm), clear wood (i.e., without knots, gross grain deviation or other structural features) is usually modelled as a homogeneous and continuous material. Moreover, the geometry and the arrangement of the wood cells within a tree, allow the definition of three local axes of material symmetry, so-called the Longitudinal ($L,1$), the Radial ($R,2$) and the Tangential ($T,3$) directions. The mechanical properties of wood, along these directions, are conventionally determined by carrying out several and independent mechanical tests, in which a uniform or simple strain state is assumed at the gauge section (Guitard, 1987).

Full-field optical methods of displacement or strain measurement have become very useful tools in experimental solid mechanics (Grédiac, 2004). According to the physical phenomenon involved in the measurement, these methods can be classified into white-light techniques (e.g.,

digital image correlation (Sutton, 1999) and grid methods (Surrel, 2009) and interferometric techniques (e.g., speckle and moiré interferometry (Could, 1995) and shearography (Lee, 2004)). By comparison with more conventional punctual techniques (e.g., strain gauges or extensometers) these methods have some important advantages: (i) they provide full-field data, so gradient fields can be conveniently assessed; (ii) they are contact-free. The application of optical methods to the deformation analysis of wood seems quite promising, particularly because of its inherent heterogeneity and anisotropy (Samarasinghe, 2000; Xavier, 2007). Nevertheless, a great effort still remains to be done in order to systematically use these techniques in the context of wood mechanics.

The longitudinal modulus of elasticity (E_L) of maritime pine (*Pinus Pinaster* Ait.) wood can be determined by compression test parallel to the grain. However, parasitic effects can occur when carrying out this

test, making difficult the data interpretation by conventional data reduction. They are assumed to be due to end-effects (*i.e.*, friction and damage) occurring locally at the contact between the specimen and the compression platens. The aim of this work is to study the influence of the geometry of the compression specimens, and therefore the amplitude of these end-effects, on the correct evaluation of E_L . For this purpose, parallelepiped wood specimens with different cross-section areas and lengths are proposed to be tested in compression. A stereovision system (DIC-3D) is chosen for providing the strain measurement on the surface of the wood samples, which performance is discussed in comparison to strain gauges measurements.

2– COMPRESSION TESTS

2.1 - Data reduction

The specimen used in the compression test method is a parallelepiped sample oriented longitudinally along the wood fibres (L, I). Experimentally, the tests are carried out on a universal tensile machine, with controlled displacement rate. The applied load, P , can be measured by the load cell of the testing machine. The uniform strain state at the centre of the specimen, ε_1 , can be measured by a linear strain gauge aligned with the longitudinal axis of the specimen. Thus, according to the linear elastic constitutive law, the longitudinal modulus of elasticity can be determined from those measured by:

$$E_1 = \frac{P/A}{\varepsilon_1} \quad (1)$$

where A is the initial cross-section area of the specimen.

2.2 - Stereovision measurements

2.2.1- *On the choice of the optical technique*

The mechanical model of the compression test assumes a homogeneous strain field at the centre of the specimen, which can be experimentally measurable by a strain gauge.

However, at the scale of observation, full-field measurements (*i.e.*, kinematic information across a region of interest covering several annual rings) can provide a more reliable strain measurement than the one obtained from a strain gauge, since the latter, covering only few annual rings, can be more prone to the local material heterogeneity (earlywood and latewood constituents). Besides, because several specimens per configuration were to be tested, the use of an optical method represented here a more inexpensive alternative.

The digital image correlation method was chosen in this work. On the one hand, this white-light technique is more easily coupled with conventional apparatus, such as a universal testing machine, than an interferometric counterpart (namely because no specific equipments, such as a laser or an anti-vibration table, are required). On the other hand, considering the biological nature of the material, this technique has the advantage of being non-intrusive and requires simpler specimen preparation (speckle pattern) than other white-light techniques such as, for instance, grid methods (Surrel, 2009; Xavier, 2007). Moreover, the utilisation of a stereovision system (3D-DIC) was advantageous in practice because: (i) there is more flexibility in the set-up (alignment and positioning) of the optical system with regard to the specimen surface; (ii) a measurement volume surrounding the region of interest of the specimen is defined through the calibration procedure of the stereovision system, so specimens can be tested sequentially afterwards, providing that they fit into this volumetric space. When compared to a monovision system (DIC-2D), however, the main disadvantage is the fact that the uncertainty on the evaluation of the parameters of the camera model represents an additional uncertainty on the displacement measurement, and therefore on the evaluation of the material parameters.

2.2.2 - *Principle*

The stereovision or 3D digital image correlation method (3D-DIC) is a full-field technique for measuring the 3D (in-plane

and out-of-plane) displacement/strain fields of a given 3D object, by analysing the sequence of the pair of stereo images recorded while the object is subjected to an external loading. A binocular stereovision (a measuring system with a pair of left and right cameras) is used for assessing the position of a 3D point in space (with regard to a given world coordinate system) from the knowledge of its stereo projection points in the two recorded images (Fig. 1). This process is known as triangulation (Hartley and Sturm, 1997). On the one hand, this method requires a camera calibration consisting in determining the extrinsic (the relative position and orientation of the coordinates systems associated to the two cameras) and intrinsic parameters of the camera model. On the other hand, a correspondence of the projection points on the two cameras must be established (stereo-matching problem) using for instance the epipolar constant concept. For a more complete description, a survey of the stereovision - 3D digital image correlation technique can be found in (Orteu, 2009).

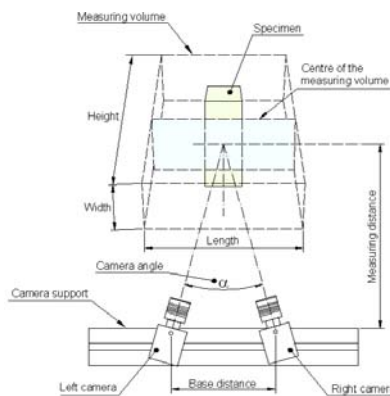


Fig 1 - Schematic representation of the stereovision measurements (Aramis®)

3-EXPERIMENTAL WORK

3.1 – Material and specimens

The wood specimens tested in this work were cut from quarter-sawn and plain-sawn boards of a single *P. pinaster* tree (geographic origin: Portugal). These boards were dried in a kiln and left afterwards in

open air during several weeks in order to reach a moisture content of about 12%. Parallelepiped specimens, oriented along the grain, were cut at the outermost part of these boards (mature wood) with different cross-section areas ($R \times T = 20 \times 20$, 30×30 and 40×40 mm²) and lengths ($L = 30$, 60 and 120 mm) (Fig 2). For the sake of repeatability, a total of 15 specimens per configuration were manufactured in a total of 135 specimens (3×3 series).

The temperature and the relative humidity of the environment during testing were around 23°C and 50%, respectively. The actual dimensions and weight of each specimen were measured before testing. The moisture content of the specimens was about 10%, determined by the oven-dry method (ASTM D 4442). The oven-dry density of the specimens (*i.e.*, the ratio between the oven-dry weight and the green volume) was in the range of 0.428 to 0.591 g/cm³.

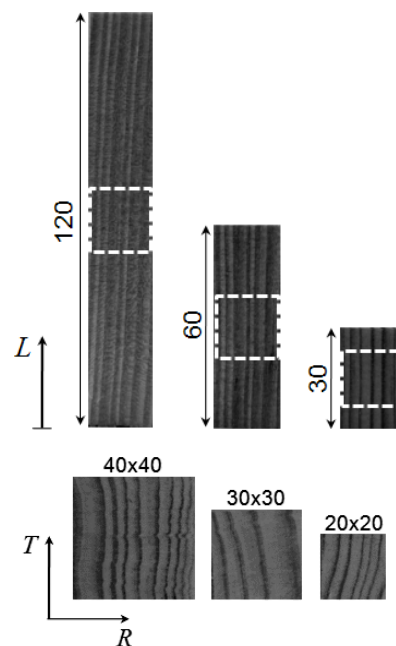


Fig 2 – Wood samples for the compression tests

3.2 - Stereovision measuring system

3.2.1 - *Set-up and calibration*

The ARAMIS stereovision system by Gesellschaft für Optische Messtechnik (GOM) (www.gom.com) was used in this work. This measurement system is

equipped with two 8-bit Baumer Optronic FWX20 cameras (resolution of 1624×1236 pixels, pixel size of $4.4 \mu\text{m}$ and sensor format of $1/1.8''$) coupled with two Schneider-Kreuznach Componar-S 50mm $f/2.8$ lenses. For mobility and adaptability, the support of the cameras was mounted on a Foba ALFAE tripod, which was positioned facing the testing machine (Fig. 3(a)). The photo-mechanical set-up was adjusted as follows:

- Firstly, the optical system was positioned with regard to a specimen mounted into the mechanical set-up. A level ruler and a laser pointer were used to guarantee a correct alignment. Besides, for a last verification, the specimen can be replaced by a mirror and the optical system set up such that a laser beam illumination, throughout the direction of the bisecting line of the angle defined by the optical axes of the two cameras (Fig. 1), would be perfectly perpendicular to the mirror's surface. The measuring distance (defined between the specimen's surface and the support of the cameras, Fig. 1) was set in the range of 300-500 mm, depending on the size of the region of interest of the specimen to be tested. The angle defined by the two cameras (α in Fig. 1) was chosen to be 25° . The base distance (defined between the rotating axis of the supports of the two cameras, Fig. 1) was adjusted in order to have coincidence between the centre of the specimen and the centre of the images recorded by the two (left and right) cameras. The two cameras were then focused, setting the lens aperture to $f/2.8$ to minimise the depth of field. The aperture of the lenses was then slightly closed ($f/11$) in order to improve the depth of field during calibration and testing. The shutter time was set to 100 ms, according to the cross-head displacement rate during testing (2 mm/min) and the size of the camera unit cells ($4.4 \mu\text{m}$). The light source was finally adjusted in order to guarantee an even illumination of the specimen's surface and to avoid over-

exposition (*i.e.*, the saturation of pixels over the field of view).

- The stereovision system must be calibrated before testing using a calibration object whose dimensions should be similar to that of the region of interest. Therefore, for the regions of 20×20 , 30×30 and $40 \times 40 \text{ mm}^2$ (Fig. 2), the calibration panels of 15×12 , 25×20 and $35 \times 30 \text{ mm}^2$ were respectively used. In the first step, the calibration object was positioned into the mechanical set-up, with special attention to its coplanarity with regard to the geometrical plane that will be defined by the specimens's surface afterwards (see Fig. 1). The calibration process is based on a set of images, taken successively by translating and rotating the calibration object with regard to the optical system. This leads to the definition of a measurement volume (Fig. 1), within which the specimens must be located afterwards. After the alignment and the calibration of the optical system, the specimens can be mounted into the mechanical set-up and tested sequentially.

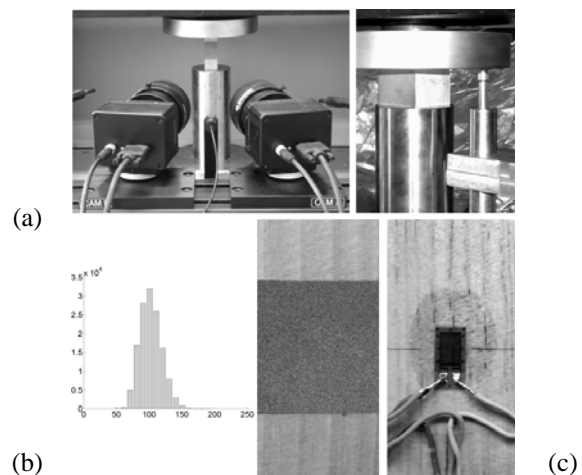


Fig 3 - (a) Photomechanical stereovision set-up; (b) speckle pattern; (c) specimen instrumented with a strain gauge

3.2.2 *Specimen preparation: speckle pattern*

The digital image correlation method is based on the assumption that the surface to be analysed has a textured pattern such that the

light intensity, diffusely reflected over the surface, will vary continuously with a suitable contrast. Different techniques have been successfully used for the creation of such a speckle pattern, employing spray or airbrush paint, toner powder deposit or lithography (Sutton *et al.*, 1999). In this work, the speckle pattern was created by applying a thin coating of white spray paint over the region of interest of the specimens followed (after drying) by a spread distribution of spots of black spray paint (Fig. 3 (b)).

3.2.3 Measurement parameters

For the region of interest of 20×20 , 30×30 and $40 \times 40 \text{ mm}^2$ (Fig. 2), a conversion factor of about 0.013, 0.020 and 0.027 mm/pixel, was respectively defined (Table 1).

In the digital image correlation method, the displacement field is measured by analysing the geometrical deformation of the images of the surface of interest, recorded before and after loading. For this purpose, the initial (undeformed) image is mapped by square facets (correlation windows), within which an independent measurement of the displacement is calculated. Therefore, the facet size on the object's plane will characterise the displacement spatial resolution. The facet step (*i.e.*, the distance between adjacent facets) can also be set either for controlling the total number of measuring points over the region of interest or for enhancing the spatial resolution by slightly overlapping adjacent facets. Typically, a great facet size will improve the precision of the measurements but also will degrade the spatial resolution (Lecompte *et al.*, 2006); thus, a compromise must be found according to the application to be handled. In this work, a facet size of 15×15 pixels was chosen, attending to the size of the region of interest, the optical system (magnification) and the quality of the granulate (average speckle size) obtained by the spray paint (Table 1). It should be said that the average size of the speckle pattern must be a few times smaller than the facet size in order to guarantee the correct computation. The facet step was also set to 15×15 pixels (Table 1), in order to avoid statistically correlated measurements.

The in-plane displacements were then numerically differentiated in order to determine the strain field needed for the material characterisation problem (Table 1).

3.2.4 Verification tests

3.2.4.1 Static tests

A static test (*i.e.*, motionless test) was performed consisting of taken several images of a target textured surface, without applied any deformation. By processing these images in order to estimate the 3D full-field displacements, both the systematic error and the accuracy of the stereovision (3D DIC) method can be assessed. The results from this study are summarised in Fig. 4. The calculated displacement maps, *e.g.*, the U_Y displacement shown in Fig. 4 (a), follows the trends of a Gaussian normal distribution, as it can be seen in the histogram plot of Fig. 4 (b). The mean value over the whole field was used to access the systematic (bias) error of the method. Typically values in the range of 0.15-0.32 μm were determined for U_X and U_Y , whereas values around 0.50 μm was reached for the U_Z component. The standard deviation on the data quantifies the accuracy of the method. For the U_X and U_Y displacements, a value of about 0.16 μm was obtained, although a higher level of 0.75 μm was observed for U_Z .

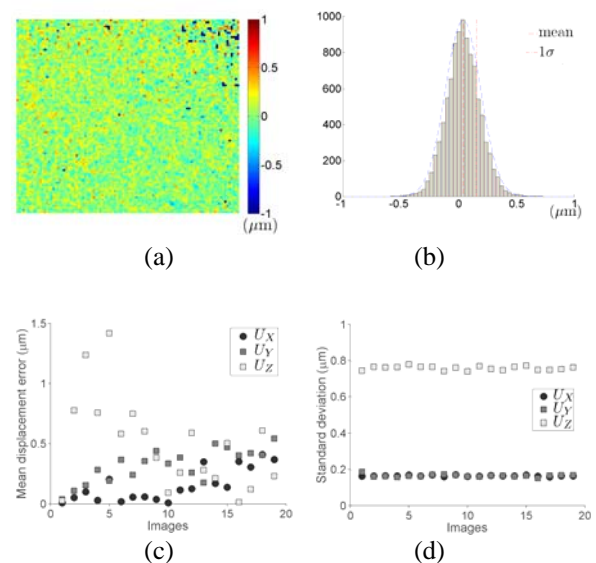


Fig 4 - Static tests: (a) U_Y displacement field; (b) U_Y histogram; (c) displacement mean (systematic) error; (d) standard deviation (accuracy)

Table 1: Parameters used in the ARAMIS-GOM software.

Project parameter - Facet	
Facet size	15 pixels
Step size	15 pixels
Project parameter - Strain	
Computation size	3
Validity code	55%
Strain computation method	Total
Stage parameter	
Accuracy	0.04 pixels
Iteration limit	Enabled
Residual gray scale level	20 Gray levels
Intersection deviation	0.3
Acquisition frequency	0.2 Hz

3.2.4.2 Rigid-body translation tests

A sample was mounted on a micrometer plate (resolution of about 1 μm) in order to perform controlled translation tests for the evaluation of the accuracy of the stereovision system. A sequence of images was recorded by applying successive translation increments along the X and Z directions of 0.001 mm up to 0.03 mm. From the optical set-up a conversion factor of 0.017 mm/pixel was determined (a ruler imaged over the field of view was used for this calculation).

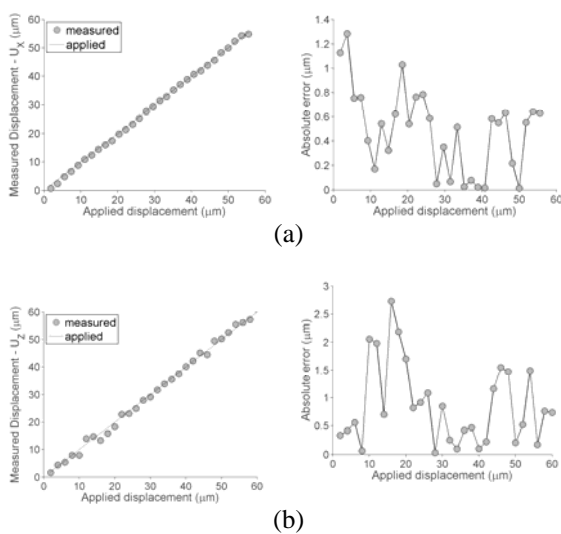


Fig 5 - Rigid-body translation tests: measured and absolute error of the (a) U_x and (b) U_z displacements as a function of the applied controlled translation (step increment of 2 μm - 0.02 pixels)

This means that each translation increment corresponds to about 0.056 pixel. For each displaced image, the average and standard deviation values over the whole calculated displacement field were evaluated (Fig 5). As it can be seen, the calculated displacements are in relatively good agreement with the actual applied translation.

3.3 Compression tests parallel to the grain

The compression tests were carried out on an Instron 1125 universal testing machine under displacement control at a rate of 2.5 mm/min. The load was measured by a 100 kN load cell. The displacement of the compression plate was measured by a LVDT (Fig. 3 (a)). In order to validate the measurements provided by the ARAMIS stereovision system, two specimens per configuration were also instrumented with strain gauges (Vishay Micro-Measurements, type EA-06-031DE-350 with a gauge grid of $3.05 \times 5.97 \text{ mm}^2$), glued on the back face of the one painted with the speckle pattern (Fig 3(c)). The M-Bond AE-10 adhesive was used for the gauge fixing. Images were grabbed during the tests with a frequency of 0.2 Hz – the synchronisation with the load recording was achieved through a trigger box – (Table 1). The data (load, LVDT and the linear strain measurement) were recorded by a HBM SPIDER 8 acquisition system. Before testing, the specimens were loaded and unloaded five times up to a force of about 500 N, in order to accommodate the specimens into the grips.

4 - RESULTS AND DISCUSSION

4.1 – Comparison with strain-gauge measurements

In order to validate the stereovision measurements, a comparison with regard to

strain gauge measurements was carried out. The summary of this study is presented in Fig. 6, by comparing directly the modulus of elasticity obtained from both strain measurement methods. As can be seen, statistically, the same mean value of E_L is observed from the stereovision and strain gauge measurements. Besides, a slightly higher scatter is observed for the strain gauge measurements. These results validate the full-field measurements from these compression tests.

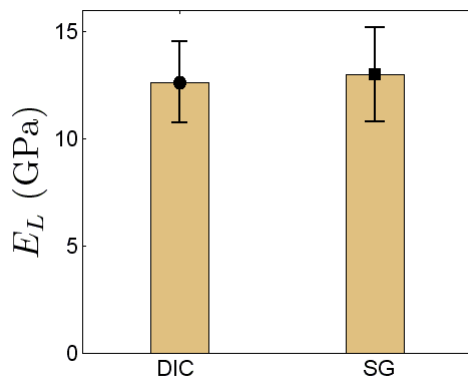


Fig 6 - Evaluation of the longitudinal modulus of elasticity from the stereovision (E_L^{DIC}) and the strain gauge (E_L^{DIC}) measurements

4.2 – Comparison of longitudinal modulus from stereovision with apparent modulus

A comparison of the apparent modulus of elasticity measured directly from the testing data (*i.e.*, load, LVDT) was performed with regard to the values obtained from the strain state measured by the full-field measurements. This study is summarised in Fig. 7, where the ratio between the modulus measured from the full-field measurements ($E_{L,DIC}$) and the LVDT ($E_{L,a}$) are plotted as function of the specimen length (h) for the different cross-section areas (*i.e.*, 20×20, 30×30 and 40×40). As it can be concluded, the apparent modulus is always lower than the elasticity modulus determined from stereovision measurements. Therefore, the apparent modulus is an underestimation of the modulus of elasticity. Clearly higher

specimen lengths and smaller cross-sections tend to reduce this discrepancy. Specifically, the cross-section of 20 × 20 mm² and specimen lengths superior to 60 mm yields more consistent apparent modulus.

The discrepancy observed between the apparent modulus and the modulus of elasticity is justified by friction and damage at the contact between the specimens and the loading platens. These end-effects become less significant if the total length of the specimens is increased and the cross section is reduced.

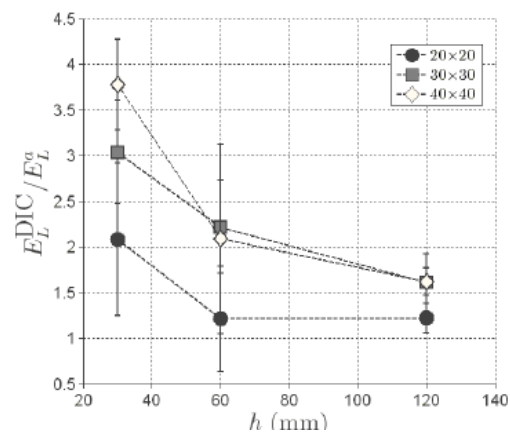


Fig 7 - Variation of the E_L^{DIC} / E_L^a ratio as a function of the geometry of the specimens (E_L^a is the apparent modulus of elasticity determined by means of the LVDT measurements)

5 – CONCLUSIONS

This work addressed the correct evaluation of the longitudinal modulus of elasticity (E_L) of maritime pine (*Pinus Pinaster Ait.*) wood by compression tests parallel to the grain. The influence of parasitic end-effect – occurring locally at the contact between the specimen and the compression platens – on the apparent E_L modulus was investigated. Different geometries of the specimens were tested in compression, by changing the cross-section area and length. The results obtained by conventional data reduction were compared to values of reference determined from full-field strain measurements provided by a stereovision technique. The stereovision strain measurements are in good agreement

with strain-gauge measurements, which is an important validation. Furthermore, stereovision strain measurements resulted in lower scatter than strain-gauge measurements.

The following main conclusions were drawn:

- specimens with short length tend to underestimate the apparent E_L modulus;
- a small cross-section area (*e.g.*, $20 \times 20 \text{ mm}^2$) leads to more accurate evaluation of the apparent E_L modulus;
- a reasonable compromise could be found for a cross-section of $20 \times 20 \text{ mm}^2$ and a length of 60 mm.

REFERENCES

ASTM D4442. Standard test methods for direct moisture content measurement of wood and wood-base materials. American Society for Testing and Materials, Philadelphia, PA, USA, 2003

Cloud, G.L., Optical methods of engineering analysis. Cambridge University Press, New York, 1995

Lee, J.-R., Molimard, J., Vautrin, A., Surrel, Y., Application of grating shearography and speckle shearography to mechanical analysis of composite material. Composites Part A: Applied Science and Manufacturing, 35(7/8):965–976, 2004

Grédiac, M., The use of full-field measurement methods in composite material characterization: Interest and limitations. Composites Part A: Applied Science and Manufacturing, 35(7/8):751–761, 2004

Guitard, D., Mécanique du matériau bois et composites, Cepadues-Editions, Collection Nabla, 1987

Hartley, R.I., Sturm, P. Triangulation. Computer Vision and Image Understanding, 68(2): 146-157, 1997

Orteu, J.-J., 3-D computer vision in experimental mechanics. Optics and Lasers in Engineering, : 47(3/4): 282-291, 2009.

Samarasinghe, S., Kulasiri, G.D., Displacement fields of wood in tension based on image processing. Part 1: Tension parallel- and perpendicular-to-grain and comparisons with isotropic behaviour. Silva Fennica, 34(3):251–259, 2000

Surrel, Y., Fringe analysis, In P.K. Rastogi, editor, Photomechanics (Topics in Applied Physics), pages 57–104. Springer Verlag, 1999

Sutton, M.A., McNeill, S.R., Helm, J.D., Chao Y.J., Advances in two-dimensional and three-dimensional computer vision. In P.K. Rastogi, editor, Photomechanics (Topics in Applied Physics), pages 323–372. Springer Verlag, 1999

Xavier, J., Avril, S., Pierron, F., Morais, J., Novel experimental approach for longitudinal-radial stiffness characterisation of clear wood by a single test, Holzforschung 61(5): 573–581, 2007